



Research Article

Effect of electrophoretic deposition kinetic behavior on dielectric property of epoxy coatings under different n-methylethanolamine's volumes

Nurhaliana Shazwani Mohd Halim¹, Norshazlina Romzei², Monisha Vani Siva Kumar², Kok-Tee Lau^{2*}, Kelly Tau Len Yong³, Umar Al-Amani Azlan², and Ah Heng You⁴

¹Fakulti Teknologi dan Kejuruteraan Mekanikal, Universiti Teknikal Malaysia Melaka, Hang Tuah Jaya, 76100 Durian Tunggal, Melaka, Malaysia

²Fakulti Teknologi dan Kejuruteraan Industri dan Pembuatan, Universiti Teknikal Malaysia Melaka, Hang Tuah Jaya, 76100 Durian Tunggal, Melaka, Malaysia

³Process Engineering Technology Section, Universiti Kuala Lumpur Malaysian Institute of Chemical and Bioengineering Technology (UniKL MICET), 78000 Alor Gajah, Melaka, Malaysia

⁴Faculty of Engineering and Technology, Multimedia University, Jalan Ayer Keroh Lama, 75450, Bukit Beruang, Melaka, Malaysia.

*Corresponding author: ktlau@utem.edu.my

Received: 12 September 2024; Revised: 29 November 2024; Accepted: 6 December 2024; Published: 15 February 2025

Abstract

This study investigates the influence of the electrophoretic deposition current–time profile on the dielectric properties of diglycidyl ether of bisphenol A (DGEBA) epoxy coatings applied via electrophoretic deposition (EPD) under varying volumes of N-methylethanolamine (MEA). Three cationic DGEBA suspensions were synthesised by mixing commercially available DGEBA with different volumes of MEA (0.5, 1.0, and 1.5 ml) as the cationisation agent. The EPD processes using these suspensions were monitored by recording the electric current versus deposition time profiles. After curing, the deposited coatings were characterised using electrochemical impedance spectroscopy, field-emission scanning electron microscopy, and energy-dispersive X-ray spectroscopy analysis. The results demonstrate that varying MEA volumes lead to distinct electric deposition current–time profiles, subsequently affecting the coating thickness and dielectric properties. The smooth exponential decay of the electric deposition current–time profile observed during EPD with the 0.5 ml MEA suspension resulted in a high coating thickness and enhanced dielectric properties. Understanding the impact of the electric deposition current–time profile on epoxy coatings deposited via EPD offers an initial quality screening tool to identify poor-quality epoxy coatings with low dielectric properties

Keywords: electrophoretic deposition, dielectric property, epoxy resin, functionalization, secondary amine

Introduction

Epoxy resins are widely used as coatings due to their stable chemical characteristics, superior electrical insulation resistance, excellent adhesion, high tensile strength, and flexural strength [1, 2]. The global market for epoxy resin is driven by increasing demand in industries such as civil engineering, chemical, and aerospace [2]. Most epoxy resins available today are DGEBA polymers. According to Jin et al. [3], when DGEBA polymers are combined with a curing agent, they undergo a curing process that transforms them into a thermosetting polymer. Curing agents such as amines, alkalis, anhydrides, and catalytic curing agents initiate and control the crosslinking of epoxy

functional groups. **Figure 1** illustrates the chemical structure of DGEBA. A key feature of the DGEBA epoxy polymer is the epoxide (oxirane) functional group, which consists of a three-membered ring containing two carbon atoms and one oxygen atom. Due to the difference in electronegativity between carbon and oxygen, the carbon atoms in this ring are electrophilic. This ring structure, characterised by its high internal strain, is significantly more reactive than typical ethers.

Cationic epoxy resins have attracted significant researchers' attention due to their unique response to applied electric fields, offering promising applications

in coating processes such as EPD [2, 3]. The synthesis of these resins involves the cationisation of the epoxide groups to achieve the desired cationic properties for EPD and curing processes. EPD is preferred over other coating methods due to its ability to deposit a uniform polymer coating thickness on targeted metallic surfaces, adaptability to new coating formulations, and suitability for various surface materials and shapes [2]. Among these formulations, an epoxy coating filled with hexagonal boron nitride particles provides metallic surfaces with electrical insulation while facilitating heat dissipation. It is suitable for electronic components, circuit boards, and other applications that require thermal management without electrical leakage.

Amine-type curing agents are among the most commonly available and widely used in the market for epoxy resins. The impact of varying amine volumes on epoxy coatings can differ significantly based on the type of amine used (primary, secondary, or tertiary) and the parameters for cationic DGEBA synthesis and EPD. These combinations result in varied coating thickness and other physical properties. Generally, the volume of amines affects both the curing process and the degree of crosslinking in the coating. For instance, Mora et al. [4] employed density functional theory to study the epoxy-amine curing mechanism and found that secondary amines react more rapidly than primary amines, thereby influencing the efficiency and characteristics of the curing process. **Figure 2** shows the molecular structure of the secondary amine N-methylethanolamine (MEA).

In the EPD process described by Kalinina and Pikalova [5], charged particles suspended in a liquid medium are attracted to and deposited onto an electrode under the influence of an electric field. These charged particles are typically cationic DGEBA polymers and free amines dispersed in a liquid medium containing solvents and additives for epoxy-based EPD suspensions. Epoxy suspensions modified by higher MEA volumes are expected to contain higher levels of free MEAs. During EPD, the cationic DGEBA and free MEAs move at different speeds toward the substrate, also known as the working electrode. Each EPD process uses epoxy suspensions with different MEA volumes to create a unique distribution of cationic epoxy polymer and free MEA deposits. After deposition on the substrate, these amines react in various ways with the epoxy functional groups to initiate crosslinking, resulting in a solid and durable epoxy coating with distinctive dielectric properties. Thus, it is believed that the EPD kinetics, as reflected in the deposition current-time profile, can affect the coating's thickness, uniformity,

and adhesion, which, in turn, influence its dielectric properties [6].

This study investigates the relationship between the EPD current-time profile and the dielectric properties of the electrodeposited epoxy coating, providing an initial quality screening tool to identify poor-quality epoxy coatings with low dielectric properties. Additionally, the study proposes a simplified chemical route to cationic DGEBA polymer formation, which is crucial for understanding and elaborating on the behaviour of cationic DGEBA synthesised using different MEA volumes.

Materials and Methods

Cationisation process of DGEBA

A commercially available DGEBA, identified as Auto-Fix 8800-A from Chemibond Enterprise, was used as the starting material for the cationisation reaction process. The as-received DGEBA liquid has a density of 1.13 g/mL, an epoxide equivalent weight (EEW) of 198–205 g/eq, and a dynamic viscosity ranging from 500 to 1,000 centipoise [7]. Cationic DGEBA epoxy resin suspensions were synthesized by a chemical reaction with six reagent-grade chemicals, including MEA, as detailed in **Table 1**. The formulations of the chemical reactants and the heating profile were adapted from the methodologies described by Bosso et al. [8] and Wismer et al. [9].

Initially, the DGEBA liquid and other components (items 2-4) were mechanically stirred in a jacketed glass reactor, which was heated by a connected heating circulator. The mixture was maintained at a temperature of 130°C for 2 hours and 50 minutes under an inert environment, created by a consistent nitrogen gas flow (10 mL/min, 99.9% purity) into the reactor, which removed the air and minimized oxidation and reduced unwanted reactions. Despite being initially immiscible, the mixture became homogeneous with continued stirring and heating. After this period, the mixture was cooled at 70°C-92°C before gradually adding MEA and the remaining chemicals (items 6-7 in **Table 1**). The amount of MEA varied from 0.5 to 1.5 mL to produce three cationic epoxy suspensions. MEA served as a cationisation agent to generate a cationic DGEBA suspension. After adding all components, the heating circulator was turned off to commence the natural cooling process, which took approximately 2-3 hours. Mechanical stirring and nitrogen flow continued until the cationic epoxy suspension reached room temperature. The suspensions were used for the coating process within a week after the cationisation process to minimise oxidation of the synthesised cationic epoxy suspensions.

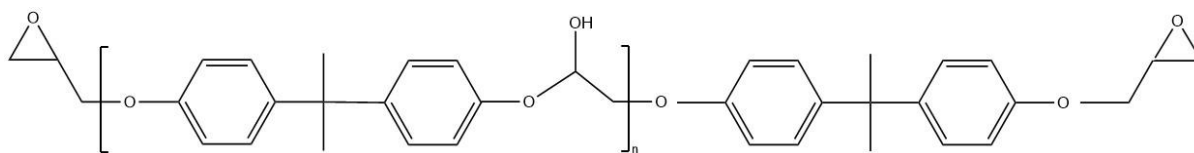


Figure 1. Molecular structure of DGEBA epoxy polymer

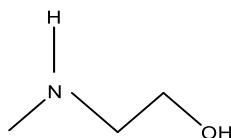


Figure 2. Molecular structure of as-received secondary amine (N-Methylethanolamine, MEA)

Table 1. Chemical reactants and amount

No	Chemical Reactant	Quantity (mL)
1	Epoxy Resin	140
2	Dimethylether of diethylene glycol (Solvent)	20
3	Monoalcohol A (1- Octanol)	41
4	Stannous Chloride	1.5 (unit in gram)
5	N-Methylethanolamine (MEA)	0.5, 1.0 and 1.5
6	Deionized water	60
7	Formic acid	0.1

Electrophoretic deposition and curing process of DGEBA coating

EPD employs two galvanised steel plates (thickness = 0.14 mm) as the anode and cathode, arranged in parallel with a 10 mm separation. Both electrodes, submerged 30 mm deep in the prepared cationic epoxy solution, facilitated the deposition process. Three distinct cationic epoxy solutions (detailed in **Table 2**) served as EPD suspensions. Deposition was performed at varying voltage levels (30, 40, and 60 V) for 15 minutes.

The EPD setup includes a DC power supply (model E3643A, with voltage range of 0–35 V or 0–60 V and current ranges of 1.4 A or 0.8 A), a digital multimeter (DMM, model 34465A), four probe wires, Keysight software for real-time monitoring of DMM readings, and a beaker containing 50 mL of the as-prepared water-based cationic epoxy resin. The Keysight software visualises the EPD graph upon completing the 15-minute deposition. Nine coated samples were obtained from the EPD process and cured in a dry oven at 100°C for 24 hours.

The electrical conductivity of the EPD solutions was measured immediately before and after the EPD process using a standard conductivity meter (model: 123-8777, brand: RS PRO).

Characterisations of epoxy coating

All characterisations of the cured epoxy coatings were carried out under standard room temperature and pressure conditions. The surface morphologies of the epoxy coating samples were analysed using field-emission scanning electron microscopy (FESEM) and Energy Dispersive X-ray Spectroscopy (EDS) with a Hitachi High-Tech SU5000 instrument. The coating samples were coated with a thin layer of gold-palladium (Au-Pd) through sputtering to improve conductivity for FESEM imaging. Electrochemical Impedance Spectroscopy (EIS) was performed to evaluate the dielectric properties of the cured epoxy coating using a Gamry Instruments Reference 600 potentiostat. EIS measurements were taken across alternating current frequencies ranging from 1 to 100,000 Hz. The real (Z') and imaginary (Z'') impedance data obtained from the EIS measurements were converted into dielectric constants (ϵ) using the method described by Joshi et al. [10]. Before the characterisation, the cured epoxy coating on the galvanised iron substrate was cut into 24 mm diameter discs and sandwiched between two spring-loaded stainless-steel electrodes. These discs were placed into a customized EIS sample holder with an effective diameter of 18 mm. The EIS data analysis was conducted based on methodologies outlined by Koh et al. [11].

Table 2. EPD Parameters for in an ambient and with nitrogen environment

No.	Volume of MEA (mL)	Voltage Levels (V)
1	0.5	30, 40, 60
2	1.0	30, 40, 60
3	1.5	30, 40, 60

Results and Discussion

Field emission scanning electron microscopy

Figure 3 illustrates the surface microstructure of coatings deposited at 30, 40, and 60 V during the EPD process using cationic DGEBA suspensions derived using different MEA volumes (0.5, 1.0, and 1.5 mL). The surface images show that all DGEBA coatings exhibit a uniform but rough microstructure. DGEBA debris is visibly dispersed within the coating and on its surface. However, the amount of DGEBA debris is reduced in the thinner 1.0 mL MEA sample. The 1.5 mL MEA sample, with an even lower coating thickness, results in a smoother surface with even less debris. The epoxy debris is suspected to originate from the fracture of residual epoxy layers formed on the glass reactor wall during the cationic epoxy synthesis process.

Table 3 presents the data on the EDS coatings produced with different amine volumes during the EPD process at 60 V. The analysis reveals that carbon is the primary coating component, consistently representing the highest percentage among the detected elements. Specifically, the carbon content exceeds 80% for all coatings, except for the 1.0 mL MEA sample deposited at 60 V. However, the nitrogen

and oxygen levels in the DGEBA coating decrease as the MEA volume increases from 0.5 to 1.5 mL, indicating the formation of a thinner DGEBA coating at higher MEA volumes. Nevertheless, an abnormal increase in oxygen content in the coating deposited using 1.0 mL of MEA suggests the possible occurrence of epoxy polymer oxidation. A comparison of the cationisation process under inert nitrogen and ambient air environments shows that oxygen content in epoxy coatings from ambient air samples is generally higher than in samples from inert nitrogen environments [12].

Calculated thickness of deposited epoxy coating

Figure 4 presents the calculated thicknesses of epoxy coatings deposited using epoxy suspensions modified by varying MEA volumes. Thickness measurements, determined using the method detailed in previous study [13], reveal a trend where coating thickness decreases as MEA volume increases. Specifically, as the MEA volume rises, the deposited epoxy coating on the galvanised iron substrate becomes progressively thinner, indicating an inversely proportional relationship between MEA volumes and coating thickness.

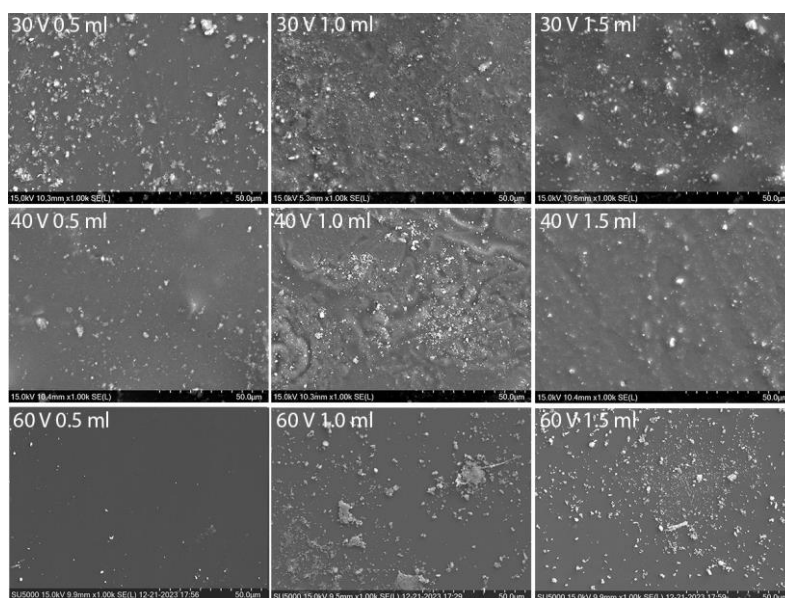
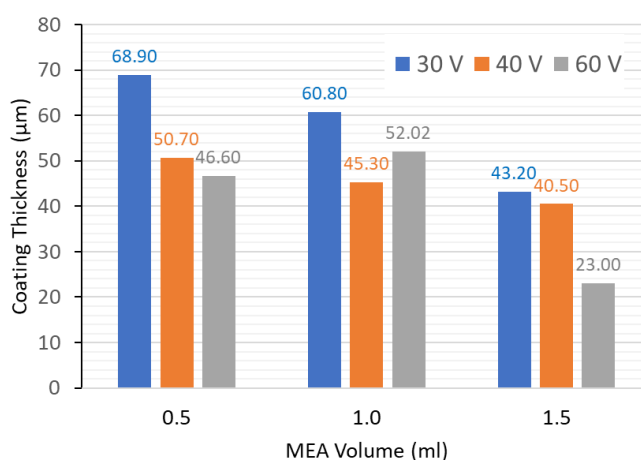


Figure 3. FESEM micrographs of surface microstructure of epoxy coating obtained at 30, 40 and 60 V using MEA volume of: (a) 0.5, (b) 1.0 and (c) 1.5 mL

Table 3. EDS data of epoxy coatings deposited at different voltages using EPD suspensions synthesised using 0.5, 1.0- and 1.5-mL MEA

Applied Voltage (V)	MEA Volume (mL)	Element (at%)		
		Carbon	Nitrogen	Oxygen
30	0.5	81.0	3.1	15.8
	1.0	83.0	3.4	13.6
	1.5	82.6	2.3	15.1
40	0.5	82.7	3.1	14.2
	1.0	83.8	2.7	13.5
	1.5	84.4	2.2	13.4
60	0.5	80.2	4.1	15.7
	1.0	75.4	1.5	23.2
	1.5	91.4	0.0	8.6

**Figure 4.** Calculated thickness of epoxy coating obtained using different MEA volumes and deposition voltages

Deposition current-time profile and EPD Suspension's electrical conductivity

Figures 5, 6, and 7 show the effect of different MEA volumes on the EPD current profile over time for cationic epoxy resin applied at different EPD voltages (30, 40, and 60 V). The current profiles were measured and analysed to understand how the behaviour of the epoxy resin changes over the deposition time and with varying applied voltages.

For the 0.5 mL MEA samples, there is a noticeable exponential decrease in the deposition current over time for all voltages. This decline occurs due to the progressive thickening of the deposited layer, which increases resistance to the movement of charged particles [14, 15]. The most pronounced decrease occurs at 60 V, as the higher applied voltage generates a greater deposition current. However, as the MEA volume increases to 1.0 and 1.5 mL, the deposition current-time profiles deviate from the expected exponential curve for the different applied voltages.

EPD using the epoxy solution modified by 1.0 mL MEA exhibits a very low deposition current, with

values less than one-tenth of the deposition current recorded during EPD using epoxy solutions with 0.5- and 1.5-mL MEA. The low and non-exponential deposition current and the larger coating thickness (see Table 3) deposited by the 1.0 mL MEA solution suggests that the related EPD mechanism does not follow the conventional constant-voltage deposition mechanism [14].

When the epoxy suspension is modified by 1.5 mL MEA, EPD becomes less effective, as demonstrated by the significantly lower coating thickness (see Table 3). The corresponding deposition current-time profile shows pronounced fluctuations compared to profiles generated by epoxy suspensions with 0.5- or 1.0-mL MEA. This fluctuation suggests that the EPD suspension modified by higher MEA volumes creates a non-steady-state condition during deposition on the working electrode, resulting in a low deposit yield.

The electrical conductivity of the EPD solution modified by higher MEA volumes (1.0 and 1.5 mL) shows a more significant decrease after the EPD process (see Figure 8). The reduced ion concentration

in the cationic epoxy solution implies that fewer cationic epoxies remain suspended. Given the lower coating thicknesses observed with higher MEA volumes (Figure 4), the decrease in ion concentration may be attributed to the depletion of cationic epoxy polymers in the 1.0- and 1.5-mL MEA suspensions. The reduced ion concentrations and non-exponential EPD current profiles suggest a change in the EPD kinetic mechanism when using epoxy suspensions with higher MEA volumes.

Chemistry aspect of cationisation process of DGEBA Polymer for EPD

The proposed chemical route, illustrated in Figure 9,

is essential for understanding and elaborating the current experimental data because it underpins the formation of cationic DGEBA required for effective electrophoretic deposition. The chemical route demonstrates that the cationisation of the DGEBA polymer using a secondary amine (e.g., MEA) and a weak acid (e.g., formic acid) can produce cationic amine groups. However, the accuracy of this route may be limited by the absence of Nuclear Magnetic Resonance (NMR) spectroscopy data to confirm the reactions involved. Further investigation is necessary to validate the reaction mechanisms and strengthen the interpretation of the results.

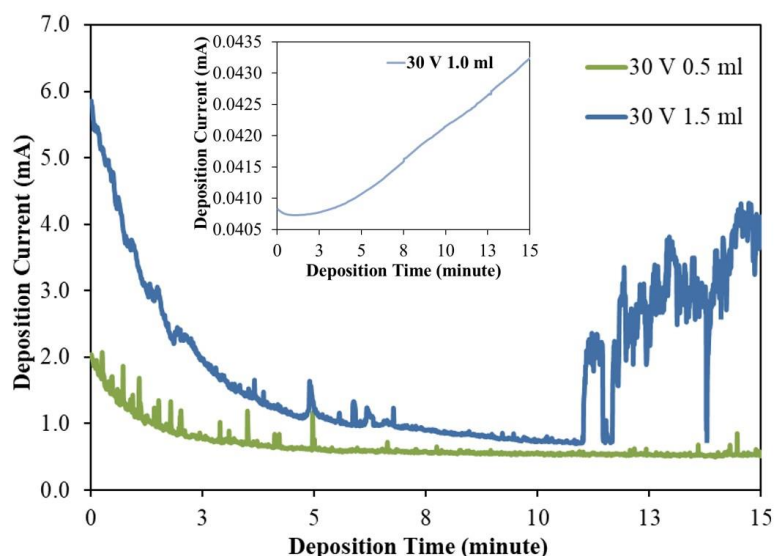


Figure 5. EPD current-time profile at 30 V when using epoxy suspension modified by different MEA volumes. *Inset:* Enlargement of EPD current-time profile using epoxy suspension modified by 1.0 mL MEA

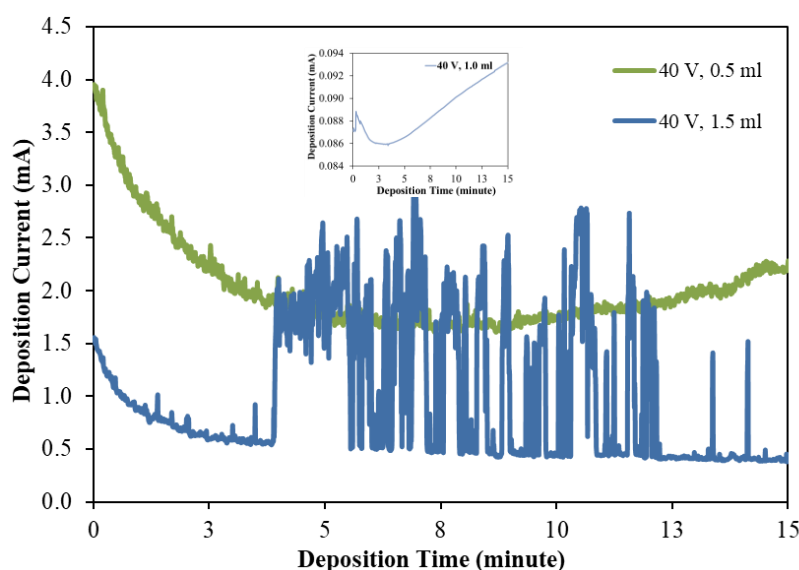


Figure 6. EPD current-time profile at 40 V when using epoxy suspension modified by different MEA volumes. *Inset:* Enlargement of EPD current-time profile using epoxy suspension modified by 1.0 mL MEA

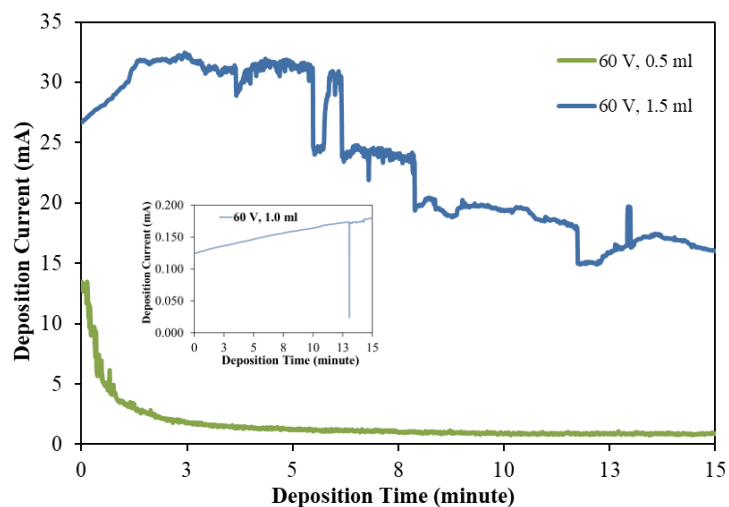


Figure 7. EPD current-time profile at 60 V when using epoxy suspension modified by different MEA volumes. *Inset:* Enlargement of EPD current-time profile using epoxy suspension modified by 1.0 mL MEA

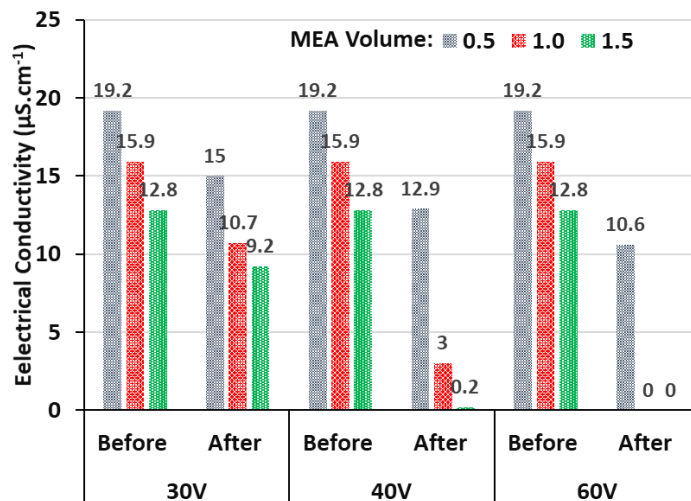


Figure 8. Electrical conductivity measurement of the EPD suspension conducted before and after EPD as function of MEA volumes

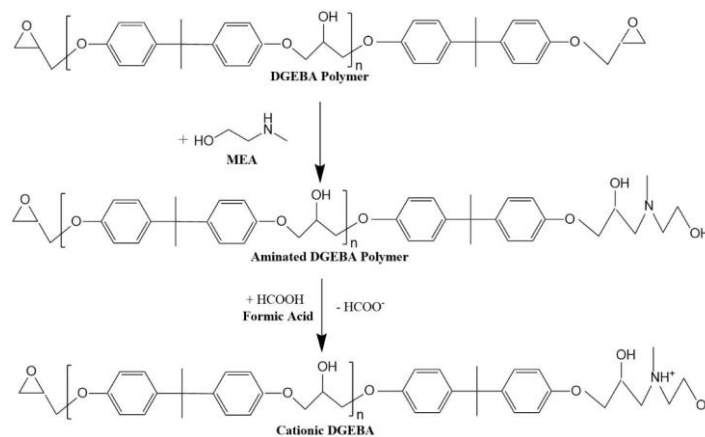


Figure 9. Simplified chemical route to cationic DGEBA polymer formation

Moreover, the proposed chemical route in **Figure 9** indicates that the secondary amine and weak acid volumes need careful adjustment to optimise the cationic DGEBA formation. If the amine volume is too low, insufficient cationic DGEBA is available for electrophoretic deposition. Conversely, excessive amine addition may convert all epoxide groups on the DGEBA into amine groups, preventing crosslinking. This effect may explain the 1.5 ml MEA samples, where coating thickness is still lower than the 0.5 ml MEA samples despite experiencing a higher EPD kinetic rate (i.e., higher deposition current, as illustrated in **Figures 5–7**).

Electrochemical impedance spectroscopy (EIS)

Figure 10 presents the Nyquist plots (Z'' vs. Z') of epoxy coatings obtained using different MEA volumes and deposition voltages. All Nyquist plots exhibit dispersion rather than a centred semicircle on the real impedance (Z') axis, indicating the real (non-Debye type) relaxation behaviour of the epoxy coatings [10, 16]. In other words, each epoxy coating sample demonstrates a distribution of relaxation times [17]. Furthermore, the non-overlapping Nyquist plots for these samples suggest different relaxation time distributions.

Epoxy resin, as a polymer with a predominantly amorphous structure, undergoes relaxation processes governed by molecular dynamics such as segmental motion and dipole reorientation, which influence its polarizability and dielectric constant [16]. Therefore, the variation in the Z'' vs. Z' relationship implies that the epoxy coatings exhibit differing molecular dynamics, largely influenced by the structure and degree of the epoxy polymer chains crosslinking [16]. **Figure 11** illustrates the decrease of dielectric constant of the epoxy coatings as the EIS frequency increases, which is consistent with findings reported by Joshi et al. [10]. Dielectric constant is calculated using the following equation:

$$\varepsilon = \frac{h}{2\pi f A \varepsilon_0} \cdot \frac{Z''}{Z'^2 + Z''^2} \quad (\text{Eq. 1})$$

Z' : real impedance of sample (Ω)

Z'' : imaginary impedance of sample (Ω)

h : sample's thickness (m)

A : sample's surface area (m^2)

f : input frequency (s^{-1})

ε_0 : dielectric permittivity of vacuum (Fm^{-1})

The frequency, f , is expressed in terms of $\log \omega$, where the angular frequency $\omega = 2\pi f$. $\log \omega$ values range from 0.998 to 5.798, corresponding to frequencies of 1 to 10,000 Hz. A decrease in the dielectric constant is

observed in epoxy coatings modified by different MEA volumes (0.5, 1.0, and 1.5 mL). The reduced dielectric property is attributed to the diminishing ability of electric dipoles to realign with the increasing frequency of the alternating current (AC) electric field during EIS testing [10]. Samples with the same material properties but greater coating thicknesses contribute to higher dielectric constants, because coating thickness is a constant factor in the dielectric constant equation (Equation 1).

At low frequencies ($\log \omega < 2.5$ or $f = 50$ Hz), the dielectric constant of the 1.5 mL MEA sample is higher than the 0.5- and 1.0-mL MEA samples when deposited at 30 and 40 V. At 30 V. The dielectric constant of the 0.5 mL MEA sample surpasses the 1.5 mL MEA sample at frequencies above 50 Hz as the dielectric constant of the 1.5 mL MEA sample decreases from 7.27 to 0.38, compared to the 0.5 mL MEA sample, which maintains a dielectric constant of 2.89 at 10,000 Hz. Among the three samples deposited at 30 V, the 1.0 mL MEA sample demonstrates a dielectric constant between 2.61 and 0.38 across the frequency range. At 40 V, the dielectric constants of the 0.5- and 1.0-mL MEA samples remain lower than the 1.5 ml MEA sample, implying a similar dielectric mechanism, particularly at frequencies above 50 Hz.

However, the 0.5 mL MEA sample consistently exhibits the highest dielectric constant at 60 V compared to the 1.0- and 1.5-mL MEA samples across the entire frequency range. The dielectric constant of the 0.5 mL MEA sample decreases from 26.28 to 5.07 across the frequency range, remaining higher than the dielectric constants of the other two samples, which fluctuate around average values of 2.38 and 2.57. The synthesised epoxy coatings demonstrate significantly high dielectric constants at frequencies below 50 Hz, particularly for coatings deposited at 40 and 60 V, but the values drop drastically to below 1.0. In contrast, previous studies on the dielectric constants of bulk DGEBA-type epoxy typically report values ranging from 4.0 to 4.8 for applied frequencies of 1 Hz to 10 GHz [18, 19], indicating that bulk epoxy exhibits a more stable dielectric constant against increasing applied frequency.

Previous research has shown that the dielectric constant of epoxy resin can be improved under increasing frequency if longer allyl chain lengths are formed after curing, provided steric hindrance does not limit the local segment mobility of the cross-linked epoxy polymer chains [19, 20]. However, the lack of a coherent trend in the dielectric constants of the samples with increasing MEA volume suggests that additional factors influence the properties.

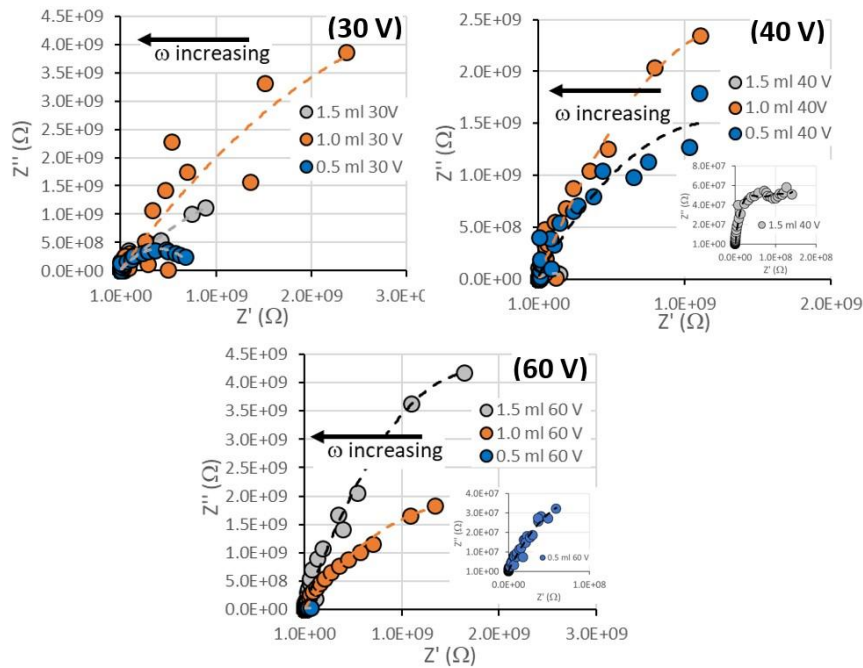


Figure 10. Nyquist plots (Z'' vs. Z') of epoxy coating obtained using different MEA volumes and deposition voltages

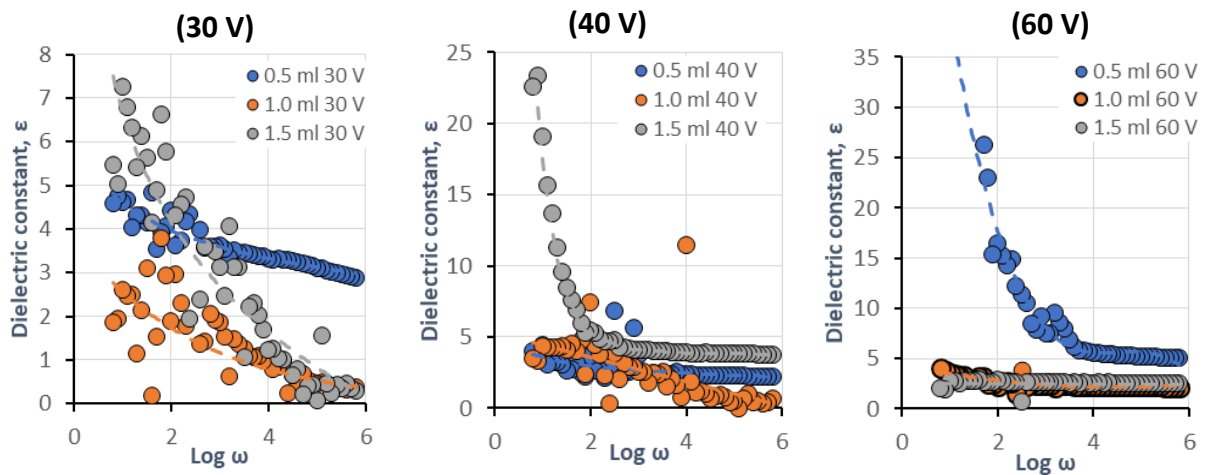


Figure 11. Graph dielectric constant, ϵ vs. $\log \omega$ of epoxy coating obtained using different MEA volumes and deposition voltages

The decrease in deposition thickness with increasing MEA volume (**Figure 4**) suggests that MEA hinders the deposition of cationic DGEBA onto the working electrode. The larger reduction in electrical conductivity after EPD in suspensions with higher MEA volumes (**Figure 8**) indicates the depletion of cationic DGEBA suspensions [21], which explains the lower deposition. However, the resulting lower coating thickness does not correspond to lower dielectric properties, as observed in the 1.5 mL MEA sample deposited at 40 V, which records a higher

dielectric constant than the 0.5- and 1.0-mL MEA samples (**Figure 11**). This suggests chemical modification of the deposited DGEBA due to electrochemical reactions during EPD.

The 0.5 mL MEA samples exhibit higher dielectric constants at different deposition voltages (30 and 60 V) than the 1.0- and 1.5-mL MEA samples. The smooth dielectric constant trend of the 0.5 mL MEA samples is supported by the normal exponential deposition current-time profile during EPD, indicating

steady-state deposition. However, the dielectric constant data for the 0.5 mL MEA sample deposited at 40 V is an outlier. The deposition current-time profile at 40 V (**Figure 6**) shows a slight increase in electric current after 8 minutes, unlike the 30 and 60 V samples, which exhibit plateau behaviour after 15 minutes.

Previous studies have reported that unstable (non-exponential) deposition currents result from conflicting deposition and electrochemical processes at the deposition electrode [22]. It is argued that the unstable current arises from the electrochemical modification of the deposited DGEBA, deteriorating the dielectric properties of the coating. Gaseous product evolution and/or water electrolysis are believed to contribute minimally to current fluctuations in the 0.5 mL MEA samples because no coating detachment was observed.

Prominent current fluctuations in the 1.5 mL MEA samples' deposition profiles suggest significant effects from electrochemical processes and gaseous evolution, resulting in lower dielectric properties. The absence of such effects in EDX data suggests further characterisation, such as X-ray photoelectron spectroscopy, is needed to investigate the electrochemical phenomena demonstrated in the deposition current-time profiles [22]. Nonetheless, the EPD current-time profile effectively identifies low-dielectric-constant samples, highlighting its potential as an initial quality screening tool for coatings with poor dielectric properties.

Conclusion

The EPD current-time profile effectively identifies low dielectric constant samples, demonstrating its potential as an initial quality screening tool to filter out coatings with poor dielectric properties. This study highlights that varying MEA volumes during the cationisation of epoxy solutions significantly affect the deposition current-time profiles, coating thickness, and dielectric properties. Specifically, higher MEA volumes result in reduced coating thickness and dielectric constant. These findings correspond with the observed deposition current-time profiles, where smoother exponential decay in the current, particularly in the 0.5 mL MEA samples, correlates with greater coating thickness and superior dielectric properties. The deposition current-time profile during EPD at 40 V exhibits a slight increase in deposition current before 15 minutes, in contrast to the 30 and 60 V samples, which demonstrate a plateau behaviour towards 15 minutes of deposition, suggesting concurrent EPD and electrochemical processes. Future studies should verify the electrochemical processes using X-ray photoelectron spectroscopy because these effects were not detected

in the EDX data.

Acknowledgement

The authors are grateful to Universiti Teknikal Malaysia Melaka for the facilities support. Special thanks to the Ministry of Higher Education for financially supporting this research under the Fundamental Research Grant Scheme (FRGS) research grant numbered FRGS/1/2022/TK10/UTEM/02.

References

1. Pourhashem, S., Vaezi, M. R., Rashidi, A. and Bagherzadeh, M. R. (2017). Exploring corrosion protection properties of solvent based epoxy-graphene oxide nanocomposite coatings on mild steel. *Corrosion Science*, 115: 78-92.
2. Xiang, Q. and Xiao, F. (2020). Applications of epoxy materials in pavement engineering. *Construction and Building Materials*, 235: 117529.
3. Jin, F.-L., Li, X. and Park, S.-J. (2015). Synthesis and application of epoxy resins: a review. *Journal of Industrial and Engineering Chemistry*, 29: 1-11.
4. Mora, A.-S., Tayouo, R., Boutevin, B., David, G. and Caillol, S. (2020). A perspective approach on the amine reactivity and the hydrogen bonds effect on epoxy-amine systems. *European Polymer Journal*, 123: 109460.
5. Kalinina, E. and Pikalova, E. (2021). Opportunities, challenges and prospects for electrodeposition of thin-film functional layers in solid oxide fuel cell technology. *Materials*, 14 (19): 5584.
6. Pingale, A. D., Owhal, A., Belgamwar, S. U. and Rathore, J. S. (2021). Effect of current on the characteristics of cuni-g nanocomposite coatings developed by Dc, Pc and Prc electrodeposition. *JOM*, 73(12): 4299-4308.
7. Chemibond, *Auto-Fix 8800-a & B: Product Information*. 2024.
8. Bosso, J. F., Burrell, L. and Wismer, M. (1974). Quaternary ammonium epoxy resin dispersion with boric acid for cationic electro-deposition. United States US-3839252-A1974.
9. Wismer, M. and Bosso, J. F. (1983). Process for the preparation of cationic resins, aqueous, dispersions, thereof, and electrodeposition using the aqueous dispersions. United States US-4419467-A1983.
10. Joshi, J. H., Kanchan, D., Joshi, M. J., Jethva, H. and Parikh, K. (2017). Dielectric relaxation, complex impedance and modulus spectroscopic studies of mix phase rod like cobalt sulfide nanoparticles. *Materials Research Bulletin*, 93: 63-73.
11. Koh, R. E., Sun, C. C., Yap, Y. L., Cheang, P. L.

- and You, A. H. (2021). Investigation of lithium transference number in pmma composite polymer electrolytes using Monte Carlo (MC) simulation and recurrence relation. *Journal of Electrochemical Science and Technology*, 12(2): 217-224.
12. Mohd Halim, N. S., Mohd Saed, M. A. A., Nik Abd Rashid, N. A. L. H., Lau, K.-T., Tau, L.-K. Y., Azlan, U. A.-A., and Nakaruk, A. (2024). Dielectric property of epoxy coating deposited using electrophoretic deposition suspension synthesised under ambient and inert atmospheres. *Journal of Advanced Research in Micro and Nano Engineering*, 24(1): 35-45.
 13. Lau, K.-T. and Samsudin, S. (2022). Electrophoretic deposition of hexagonal boron nitride particles from low conductivity suspension. *Journal of Science and Technology*, 30(2): 1237-1256.
 14. Sarkar, P. and Nicholson, P. S. (1996). Electrophoretic deposition (Epd): Mechanisms, kinetics, and application to ceramics. *Journal of the American Ceramic Society*, 79(8): 1987-2002.
 15. Hajizadeh, A., Aliofkhaezai, M., Hasanpoor, M. and Mohammadi, E. (2018). Comparison of electrophoretic deposition kinetics of graphene oxide nanosheets in organic and aqueous solutions. *Ceramics International*, 44(9): 10951-10960.
 16. Vassilikou-Dova, A. and Kalogeras, I. M., Dielectric analysis (Dea), in thermal analysis of polymers: fundamentals and applications. J.D. Menczel R.B. Prime, Editors. 2009, John Wiley & Sons, Inc.: New Jersey. p. 497-613.
 17. Nioua, Y., El Bouazzaoui, S., Melo, B., Prezas, P., Graça, M., Achour, M., Costa, L. and Brosseau, C. (2017). Analyzing the frequency and temperature dependences of the ac conductivity and dielectric analysis of reduced graphene oxide/epoxy polymer nanocomposites. *Journal of Materials Science*, 52(24): 13790-13798.
 18. Lee, J., Jin, F., Park, S.-J. and Park, J.-M. (2004). Study of new fluorine-containing epoxy resin for low dielectric constant. *Surface and Coatings Technology*, 180-181:650-654.
 19. McMaster, M. S., Yilmaz, T. E., Patel, A., Maiorana, A., Manas-Zloczower, I., Gross, R. and Singer, K. D. (2018). Dielectric properties of bio-based diphenolate ester epoxies. *ACS Applied Materials & Interfaces*, 10(16): 13924-13930.
 20. Wang, Y., Du, B., Kong, X. and Li, X. (2024). Effects of cross - linked networks on dielectric properties of epoxy resins based on molecular dynamics. *Journal of Applied Polymer Science*, 141(11): e55104.
 21. Van der Biest, O. O. and Vandeperre, L. J. (1999). Electrophoretic deposition of materials. *Annual Review Materials Sciences*, 29(1): 327-352.
 22. Diba, M., García-Gallastegui, A., Klupp Taylor, R. N., Pishbin, F., Ryan, M. P., Shaffer, M. S. P. and Boccaccini, A. R. (2014). Quantitative evaluation of electrophoretic deposition kinetics of graphene oxide. *Carbon*, 67 656-661.